The non-conservative distribution pattern of organic matter in the Rajang, a tropical river with peatland in its estuary

Zhuo-Yi Zhu[1]*, Joanne Oakes[2], Bradley Eyre[2], You-You Hao[1], Edwin Sien Aun Sia[3], Shan Jiang[1], Moritz Müller[3], Jing Zhang[1]

1. State Key Laboratory of Estuarine and Coastal Research, East China Normal University, Shanghai, 200241, China

2. Centre for Coastal Biogeochemistry, School of Environment, Science and Engineering, Southern Cross University, Lismore NSW, 2480, Australia

3. Swinburne University of Technology, Faculty of Engineering, Computing and Science, Jalan Simpang Tiga, Kuching, 93350, Sarawak, Malaysia

*Corresponding author: Z.Y. Zhu, zyzhu@sklec.ecnu.edu.cn; zhu.zhuoyi@163.com

Abstract

South-east Asian peatland-draining rivers have attracted much attention due to their high dissolved organic carbon (DOC) yield and high CO_2 emissions under anthropogenic activities. In August 2016, we carried out a field investigation of the Rajang river and estuary, a tropical system located in Sarawak, Malaysia. The Rajang has peatland in its estuary, while the river basin is covered by tropical rainforest. DOC $\delta^{13}C$ in the Rajang ranged from -28.7‰ to -20.1‰, with a U-shaped trend from river to estuary. For particulate organic carbon (POC), $\delta^{13}C$ ranged between –29.4‰ and –31.1‰ in the river and there was a clear increasing trend towards more enriched $\delta^{13}C$ values with higher salinity. In the estuary, there was a linear conservative dilution pattern for dissolved organic matter composition (as quantified by D/L amino acid enantiomers) plotted against DOC $\delta^{13}C$, whereas when plotted against salinity dissolved D/L amino acid enantiomers values were higher than the theoretical dilution value. Together, these data indicate that the addition of DOC to the estuary (by peatland) not only increased the DOC concentration, but also altered its composition, by adding more bio-degraded, ^{13}C-depleted organic matter into the bulk dissolved organic matter. Alteration of organic matter composition (addition of a more degraded subpart) was also apparent for the particulate phase, but patterns were less clear. The Rajang was characterized by DOC to DON (dissolved organic nitrogen) ratios of 50 in the river section, with loss of DON in the estuary increasing the ratio to 140, suggesting unbalanced export of organic carbon and nitrogen. Under anthropogenic activities, further assessment of organic carbon to nitrogen ratios is needed.

Keyword

Amino acid enantiomers, DOC, POC, stable carbon isotope, Rajang, peatland

1. Introduction

Fluxes and cycling of organic matter (OM) in rivers and estuaries are important influences on global biogeochemical cycles and climate change. In river basins, vascular plants are the ultimate sources of organic matter (Hedges and Man, 1979), but algae, moss, and bacteria are also important (Hernes et al., 2007). As well as providing a source of OM, bacteria may strongly modify the composition of organic matter within a river and its resistance to degradation. The lability of organic matter determines how rapidly organic carbon will be transformed into inorganic carbon (CO_2), which can vary from hours to millions of years. The lability of organic matter therefore plays a role in determining whether organic matter is either a source or a sink of carbon in the atmosphere (Zhang et al., 2018). Based on ^{14}C in organic carbon, Mayorga et al. (2005) determined that the degradation of recently synthesized organic matter in the river basin was the main reason Amazonian river waters were supersaturated in CO_2, and hence a source of atmospheric CO_2. This highlights the potential importance of organic matter stability for carbon cycling within river systems. Nitrogen is another important element in organic matter, which is not independent of carbon, but instead is closely combined with carbon in various chemical compounds (like amino acids). Due to the nature of these specific compounds, the behavior of bulk carbon and nitrogen can differ substantially. In basins with peatland, the leaching of DOC is related to the status of peatland (disturbed vs undisturbed), whereas the leaching of dissolved organic nitrogen (DON) is controlled by the soil inorganic nitrogen content (Kalbitz and Geyer, 2002). The different leaching mechanisms of organic carbon and nitrogen indicates that the comparison of these two elements would deepen our understanding of organic matter cycles.

Tropical south-east Asian rivers play an important role in both dissolved and particulate organic

58　matter export (Baum et al., 2007; Huang et al., 2017; Müller et al., 2016). Located in Sarawak,

59　Malaysia (Fig. 1a), the turbid Rajang river (hereafter refer to as the Rajang) is the longest river in

60　Malaysia. The Rajang flows through tropical rainforest, and peatland and mangroves are distributed

61　in the estuary. A dam was constructed in the upper reaches of the Rajang in 2015, but the total

62　suspended matter (TSM) in the river remains at $100 - 200$ mg/L (Müller-Dum et al., 2019). This

63　terrestrial organic matter can be expected to be diluted at the adjacent coast, given that the turbidity

64　of the river strongly limits organic matter photo-degradation within the river and estuary. Fluvial

65　organic matter is therefore dominated by bacterial utilization and abiotic processes such as

66　desorption/adsorption between particulate and dissolved phases (Martin et al., 2018). Further,

67　dissolved oxygen is negatively related to pCO_2, likely due to in-stream heterotrophic respiration

68　(Müller-Dum et al., 2019). In the Rajang brackish estuary, where peatland is located, addition of

69　peatland DOC into river water is suggested by the non-conservative mixing pattern of DOC with

70　increasing salinity (Martin et al., 2018), whereas removal of DON in the Rajang estuary is suggested

71　by nitrogen stable isotopes (Jiang et al., 2019).

72　　　While stable isotopes of carbon and nitrogen are useful tools for tracing organic matter, amino

73　acids (AAs) are the most important organic carbon and nitrogen carriers that have been chemically

74　identified, accounting for up to ~100% of the particulate nitrogen in aquatic environments, and up

75　to nearly half of the particulate organic carbon pool (Jennerjahn et al., 2004). Due to the selective

76　removal and accumulation of certain amino acids, amino acids are important biomarkers in early

77　diagenesis, allowing quantification of organic matter lability/resistance (Dauwe and Middelburg,

78　1998; Kaiser and Benner, 2009). With the exception of glycine, amino acids are chiral. L forms of

79　amino acids are from animals, plants and plankton, whereas D forms mainly come from bacteria,

80   and are key chemical compounds in peptidoglycan, which forms the basic structure of bacterial cell

81   membranes (Vollmer et al., 2008). Due to the key role of bacteria in OM alteration and early

82   diagenesis, D-AAs (D forms of AAs) tend to accumulate during OM degradation. A higher ratio of

83   D- to L-AAs (D/L ratio) therefore indicates that OM is more refractory (Davis et al., 2009). As a

84   non-protein amino acid, accumulation of GABA (γ－aminobutyric acid) is also highly related to

85   OM degradation (Davis et al., 2009). Conversely, a lower D/L ratio and GABA% indicates that OM

86   is relatively less degraded, and hence more labile. In river waters, elevated D-AAs also indicate the

87   presence of soil humic substances, which are a product of bacteria and their detritus (Kimber et al.,

88   1990).

89   Tropical rivers are dominated by refractory (or bio-degraded) organic matter, yet labile OM is

90   also known to play a role in river carbon cycles (Mayorga et al., 2005). It is hence expected that

91   fluvial organic matter within a river would be a mixture of labile organic matter (which can be

92   respired to support pCO_2) and refractory terrestrial organic matter (which will be diluted/degraded

93   after entering the sea (Martin et al., 2018)), while in the estuary there would be addition of dissolved

94   OM from peatland/mangrove (Dittmar et al., 2001b; Müller et al., 2016). Previous studies of OM in

95   south-east Asian rivers mainly focused on its bulk concentrations, ages, or optical properties (Martin

96   et al., 2018 and ref. therein). The use of biomarker approaches has been very limited (Baum et al.,

97   2007; Gandois et al., 2014). Given the processes described above and their potential contribution to

98   the carbon (Müller-Dum et al., 2019) and nitrogen cycles (Jiang et al., 2019), it is somewhat

99   surprising that there has been limited application of amino acid approaches, including D-AAs, to

100   investigate organic matter composition and the role of estuarine peatland/mangrove in OM

101   regulation (Jennerjahn et al., 2004). South-east Asian rivers are subject to multiple stressors due to

102   increasing anthropogenic activities in both their riverine (e.g., damming, logging/secondary

103   plantation) and estuarine sections (e.g., drainage, and oil palm plantations) (Hooijer et al., 2015).

104   Amino acid enantiomers and carbon/nitrogen isotopes have the ability to provide molecular level

105   evidence for the impact of these stressors on carbon and nitrogen cycling and bulk biogeochemistry,

106   as well as insight into the mechanisms underlying such changes.

107   In this study, we carried out a field investigation in the Rajang in August 2016, from stations

108   S10 to S1, located on the coast of the South China Sea adjacent to the Rajang (Fig. 1b). AA

109   enantiomers and $\delta^{13}C$ values of DOC were used to elucidate the succession of organic matter

110   sources/composition from the fresh water to the estuarine sections of the Rajang. Our aim was to

111   address the following questions: 1) Given that peatland contributes additional DOC to fluvial DOC

112   (Müller et al., 2016), does the composition of dissolved OM change from river to estuary? 2) Do

113   changes in organic nitrogen mirror changes in organic carbon? 3) Hence, what is the role of

114   peatland/mangroves on OM composition and lability in the Rajang? Globally, rivers at low latitudes

115   receive much less attention relative to temperate and polar rivers (36 vs. 958 studies) (Cloern et al.,

116   2014), while they could be equally important for global carbon cycles (Cloern et al., 2014). This

117   study ultimately aims to enrich our understanding of organic carbon and nitrogen cycles in tropical

118   rivers/estuaries.

119

120   **2. Materials and methods**

121   All abbreviations, together with the amino acids measured in this study, are listed in table 1.

122   **2.1 Brief background**

123   The Rajang river and estuary is located in Sarawak, Malaysia. The climate is wet year-round,

5

124   but the main precipitation typically occurs in winter (November to February). Climate is influenced

125   by the El Niño-Southern Oscillation (ENSO) and Madden-Julian Oscillation. In August 2016, the

126   discharge was estimated as 2440 m^3/s, in comparison with an annual mean discharge of 4000 m^3/s

127   for 2016 and 2017 (Müller-Dum et al., 2019).

128   Based on salinity, station S5 is regarded as the boundary of the fresh and estuarine water of the

129   Rajang (Fig. 1b). In this work all samples with a salinity of 0 were regarded as fresh water, while

130   samples with salinity >0 were regarded as estuarine. In the estuary, there are several branches,

131   namely Igan, Lassa, Paloh, and Rajang itself (Fig. 1b). Since water in all these branches is derived

132   from the Rajang river (i.e., upstream of S5), in this study all these branches are regarded as the

133   Rajang estuary. Peatland and mangroves are common in the estuary (shown in Fig. 1b) while tropical

134   rainforest is widely distributed upstream of S5 (not shown in Fig. 1b). The peatland is under strong

135   pressure of draining and change of use for oil palm plantations, while logging and secondary growth

136   is very common in the river basin (Hooijer et al., 2015). Compared with other peatland-draining

137   tropical blackwater rivers, the Rajang is more like a turbid tropical rainforest river (Müller-Dum et

138   al., 2019), but with notable peatland/mangrove in its estuary (Fig. 1b).

139   **2.2 Field sampling**

140   The field work was carried out in August 2016. The sampling stations covered from S10 (the

141   upper most station in this study) to S1 on the coast. At each station, a pre-cleaned and sample-rinsed

142   bucket was used to collect surface water from the center of the channel in a boat. After sample

143   collection, pretreatment was done immediately on board the boat. For DOC and its stable carbon

144   isotope ratios ($\delta^{13}C$), water samples were collected by syringe filtering (pre-combusted Whatman

145   GF/F; 0.7 µm) approximately 30 ml of sample water into a pre-combusted 40 ml borosilicate vial.

146 Samples were preserved with five drops of concentrated phosphoric acid and sealed with a lid

147 containing a Teflon-coated septa. For total dissolved amino acids (TDAA), water samples were

148 filtered through a 0.4 μm nylon filter. For particulate OM samples (TSM, POC, POC-δ^{13}C, PN and

149 PN-δ^{15}N, and total particulate amino acids (TPAA)), suspended particles were concentrated onto

150 glass fiber filters (pre-combusted Whatman GF/F; 0.7 μm). The GF/F filters were folded and packed

151 in pre-combusted aluminum. All samples were immediately stored frozen (–20°C) until analysis. At

152 every station both particulate and dissolved samples were collected, but a few samples were lost

153 (broken) during transportation back to Shanghai. The lost samples were the particulate samples

154 (POC and TSM) from stations S16 (conductivity = 64 μS/cm), S4 (salinity = 4.8), S25 (salinity =

155 11.7) and S29 (salinity = 4.3), and a total dissolved AA sample (TDAA) from station S24 (salinity

156 = 19.1).   A portable meter (Aquaread, AP-2000) was used to obtain conductivity/salinity,

157 temperature, dissolved oxygen and pH.

158 **2.3 Laboratory analyses**

159 Concentrations and δ^{13}C of DOC were measured at the Centre for Coastal Biogeochemistry at

160 Southern Cross University (Lismore, Australia) via continuous-flow wet oxidation isotope-ratio

161 mass spectrometry using an Aurora 1030W total organic carbon analyzer coupled to a Thermo Delta

162 V Plus IRMS (Oakes et al. 2010). Glucose of known isotopic composition dissolved in He-purged

163 Milli-Q was used as a standard to correct for drift and to verify sample concentrations and δ^{13}C

164 values. Reproducibility for concentrations and δ^{13}C was ± 0.2 mg l^{-1} and ± 0.4 ‰. For the

165 determination of POC, samples (GF/F glass fiber filters) were freeze-dried and analyzed with a

166 CHNOS analyzer (Model: Vario EL III) after removing the inorganic carbon by reaction with HCl

167 vapor. For PN, a similar procedure was followed, with no acid treatment. The detection limit for

168   POC was 7.5×10^{-6} g, with precision better than 6%, based on repeated determinations (Zhu et al.,

169   2006). The POC-δ^{13}C and PN-δ^{15}N values were determined using a DELTA^{plus}/XL isotopic ratio

170   mass spectrometer (Finnigan MAT Com. USA) interfaced with a Carlo Erba 2500 elemental

171   analyzer. The standard for δ^{13}C was PDB and the precision of the analysis was $\pm$ 0.2‰. For δ^{15}N,

172   the standard was air and precision was $\pm$ 0.3‰.

173   Total hydrolyzable AAs were extracted and analyzed following the method of Fitznar et al., (1999)

174   with slight modifications (Zhu et al., 2014). Briefly, samples were first hydrolyzed with HCl at

175   110°C. After pre-column derivatization with o-Phthaldialdehyde (OPA) and N-Isobutyryl-L/D-

176   cysteine (IBLC/IBDC), AAs and their enantiomers were analyzed using an HPLC (Agilent 1200)

177   comprising of an online vacuum degasser, a quaternary pump, an auto-sampler, a thermostatted

178   column and a fluorescence detector (excitation 330 nm, emission 445 nm). The analytical column

179   was a Phenomenex Hyperclone column (BDS C18, 250×4mm, 5μm) with a corresponding pre-

180   column. To eliminate the influence of racemization of L-type AAs in the hydrolysis process, the

181   concentration of D/L-AAs measured in actual samples was corrected according to the formula

182   obtained by Kaiser and Benner (2005). The detection limits for glycine (Gly) and individual AAs

183   enantiomers were in the lower picomolar level. Asx and Glx were used for aspartic acid + asparagine

184   and glutamic acid + glutamine, respectively (Table 1), as the corresponding acids are formed via

185   deamination during hydrolysis.

186   A few samples (e.g., TDAA in S1 station) were not measured due to instrument hardware

187   problems. Therefore, there is not always corresponding particulate and dissolved data for some

188   stations.

189

3. Results

In August 2016, the TSM concentration in the Rajang ranged from 22 mg/L to 161 mg/L. Mean TSM concentrations in the fresh water and estuarine sections were 61 mg/L and 161 mg/L, respectively (Table 2). Throughout the system DOC concentrations exceeded POC concentrations. DOC and POC in the fresh water section averaged 337 μM and 86 μM, and in the estuarine section 345 μM and 64 μM, respectively (Table 2). DOC concentrations were slightly higher in the estuary than in the fresh water section (Table 2), and maximum concentrations for both DOC and POC were found at around salinity 15 to 20 in the estuary (Fig. 2).

DOC δ^{13}C ranged from –28.7‰ to –20.1‰ (Table 2). There was A U-shaped trend in DOC δ^{13}C from the fresh water to the estuary section can be identified for, with one outlier from the Rajang main stream at a salinity of 5 (S2 station; Fig. 3a). The minimum DOC δ^{13}C (bottom of the U) was detected at a salinity of ~10 (Fig. 3a). For particulate OM, δ^{13}C ranged between –29.4‰ to –31.1‰ in the fresh water section. In the estuary section, there was a clear increasing trend with increasing salinity, from –30‰ (S=1.1) to values close to –24‰ (S>30) (Fig. 3b).

In the fresh water section, the mean TDAA and TPAA concentrations were 0.3 μM and 2.5 μM, respectively (Table 3). For TDAA, the AA carbon yield (the carbon from AA divided by bulk DOC or POC, in %) was similar in both fresh water and estuary sections, namely 0.40% and 0.38% (mean), respectively (Table 3). In contrast, AA nitrogen yield was higher in the estuary (11%) than in the fresh water section (4.8%) (Table 3). For TPAA, there was little difference between the fresh water and estuary sections in AA carbon yield (13.5% and 16.8%, respectively) and nitrogen yield (66% and 62%, respectively) (Table 3).

In the both dissolved and particulate phase, Gly, Glx, Ala and Asx were the most abundant AA

212   compounds. These four AAs together accounted for 66% of TDAA and 47% of TPAA in the fresh

213   water section, and 59% of TDAA and 48% of TPAA in the estuary. The non-protein AA GABA

214   was detected in trace amounts, but was more abundant in the dissolved phase than in the particulate

215   phase, as indicated by the higher GABA% in the dissolved phase (Table 3). GABA% decreased

216   from 2% (fresh water section mean) to 1.3% (estuarine section mean) in the dissolved phase, and

217   decreased from 0.7% (fresh water section mean) to 0.4% (estuarine section mean) in the particulate

218   phase (Table 3). In the estuary, GABA% in the dissolved phase remained stable (~1.5%) in brackish

219   water (salinity 5 to 20) and quickly dropped to <1% where salinity was over 30 (Fig. 4a). Most of

220   the GABA% values lay above the theoretical mixing line (Fig. 4a). In the particulate phase, there

221   was an overall decrease in GABA% with increasing salinity within the estuary (Fig. 4b).

222   The percentage of D- form enantiomers of AAs in TDAA averaged 12% for both fresh water

223   and estuarine sections, with Glx and Asx being the most abundant D- form AAs. The percentage of

224   D- form AAs was much lower in TPAA, decreasing from a mean of 4.4% in the fresh water section

225   to a mean of 3.3% in the estuary (Table 3). Patterns in the variation of D/L Glx (Fig. 5) along the

226   conductivity/salinity gradient in the Rajang were similar to those for GABA% (Fig. 4) for both

227   dissolved and particulate phases. Similar to GABA%, all the dissolved samples in the estuary had

228   elevated values for D/L Glx (i.e., values above the theoretical dilution line) (Figs. 4a and 5a).

229

230   **4. Discussion**

231   **4.1 Distribution patterns of OM composition**

232   *Dissolved OM*

233   Terrestrial OM usually has a more negative $\delta^{13}C$ value (–32‰ to –26‰ for C3 plants), whereas

234　marine OM has more positive values (δ^{13}C, ~ –20‰) (Lamb et al., 2006; Mayorga et al., 2005).

235　Overall, the very negative δ^{13}C values for DOC (<–26‰) in the riverine section of the Rajang clearly

236　indicate that the OM had a C3 plant source (e.g., mangroves and oil palms (Jennerjahn et al., 2004;

237　Lamade et al., 2009; Wu et al., 2019)), whereas DOC δ^{13}C values > –24‰ in the estuary

238　(salinity >30) suggest a mixture of terrestrial and marine OM sources (Fig. 3a). The most depleted

239　δ^{13}C values for DOC occurred at a salinity of 10 (Fig. 3a). Above this salinity, the influence of

240　marine OM became more overwhelming, and the bulk DOC δ^{13}C signal was more enriched (Fig.

241　3a).

242　　　Among samples in the fresh water section, the most enriched DOC-δ^{13}C values (S10 and S15;

243　DOC-δ^{13}C: –25‰; Fig. 3a), although initially appearing to be outliers, were characterized by very

244　elevated D/L amino acids ratios (Fig. 6a). This was particularly the case for the sample from S10

245　(the upper most station in this study; Fig. 1b), which showed a maximum D/L Glx ratio of 0.57 (Fig.

246　6a). In addition, these samples from S10 and S15 also showed a higher D/L ratio for Asp (S10: 0.49,

247　S15: 0.38; figure not shown) when compared to all fresh water or estuary samples (mean: 0.34;

248　Table 3). On land, D- form amino acids can be derived from abiotic racemization. This process

249　occurs over a very long time scale (e.g., over thousands of years) and results in L- form amino acids

250　slowly changing into their corresponding D- form (Schroeder and Bada, 1976). More significantly,

251　in contemporary environments D- form amino acids are widely synthesized by bacteria during cell

252　membrane construction (Schleifer and Kandler, 1972). D/L Glutamic acid and D/L Aspartic acid

253　ratios of pure peptidoglycan (*Staphylococcus aureus*, Gram-positive) are 0.49 and 0.30, respectively

254　(Amon et al., 2001). Although δ^{13}C values for bacteria in the Rajang remain unknown, bacteria have

255　been reported to have δ^{13}C values from –12‰ to –27‰ (Lamb et al., 2006). Contribution of OM

256   derived from bacteria may therefore explain the relatively enriched $\delta^{13}C$ values observed at inland

257   station S10 and station S15. A possible OM source at these stations is soil humic substances, which

258   are expected to have a high contribution from bacteria, and therefore D-form amino acids (Dittmar

259   et al., 2001a). A more depleted pattern of DOC $\delta^{13}C$ from mountain to lowland is suggested to be

260   due to dilution and mixing with younger OM in the lowland (Mayorga et al., 2005). This is

261   consistent with the pattern we observed of depleted DOC $\delta^{13}C$ values within the fresh water section

262   corresponding with lower D/L ratios pattern, which suggests dilution with less degraded OM (see

263   orange circles in Fig. 6a). Whether the elevated D/L ratios and relatively positive $\delta^{13}C$ values for

264   dissolved samples in the fresh water section at S10 and S15 (Fig. 6a) reflect the presence of soil

265   humic substances, or instead reflect the direct presence of bacteria, requires further study.

266   In the estuarine section, it was very clear that terrestrial bio-degraded OM (indicated by

267   elevated D/L ratios and more negative $\delta^{13}C$) is diluted with more labile OM (lower in D/L ratio but

268   more positive $\delta^{13}C$) (see solid blue data points in Fig. 6a). However, this apparent dilution trend

269   became less clear or showed no trend) when D/L ratio was plotted against salinity (Fig. 5a). This

270   was also confirmed by the GABA% distribution pattern which showed a platform-like pattern at a

271   salinity between 5 and 20 (Fig. 4a). Though TDAA at S1 was missing, the composition of TDAA

272   at S2 (salinity = 31.2) was very typical of marine OM (i.e., very low D/L ratio and relatively enriched

273   DOC-$\delta^{13}C$; Fig. 6a). Hence there is a conservative distribution pattern for dissolved OM in the

274   estuary when plotted against $\delta^{13}C$ (Fig. 6a) but not when plotted against salinity (Figs. 4a&5a). The

275   location above the conservative dilution line of all OM data in the brackish estuary (salinity 10 to

276   25; Figs. 4a & 5a), indicates that the OM in the estuarine section was more degraded than

277   theoretically expected. The combination of degraded OM and DOC concentration increase in the

278   estuary (345 μM in the estuary vs. 337 μM in the fresh water section; Fig. 2b), suggests the addition

279   of degraded DOC to the Rajang. Non-conservative dissolved OM behavior in the estuary has

280   previously been reported based on an optical approach (Martin et al., 2018), and minimal OM

281   alteration during estuarine transport was suggested (Martin et al., 2018). Hence, it is likely that

282   changes in dissolved OM composition (Figs. 4a & 5a) may largely take place in land/estuary (e.g.,

283   in pore waters of soil) and impact the Rajang riverine dissolved OM via leaching from soils.

284   *Particulate OM*

285   In the river section of the Rajang, depleted POC-δ^{13}C indicated the strong influence of

286   terrestrial OM; this OM is likely derived from C3 plant material, which is a major component of the

287   sediment OM (Wu et al., 2019). In the estuarine section of the Rajang, there was seaward enrichment

288   of POC-δ^{13}C (Fig. 3b), suggesting that the OM was diluted with marine particulate OM, and aligning

289   with similar isotope enrichment of suspended particles in brackish water observed in other estuaries

290   (Cifuentes et al., 1996; Raymond and Bauer, 2001). Unlike dissolved OM, there were no POC

291   samples with unusually enriched δ^{13}C values in the fresh water section (Figs. 6b&c). D/L Glx ratios

292   of particulate OM in the fresh water section was higher when compared with that in the estuary

293   section (Table 3), and overall, when compared with dissolved OM, particulate OM basically became

294   more labile when transported seawards, as indicated by shifts in its composition   (Figs. 4b&5b)

295   and isotope ratio with salinity (Figs. 6b&c).

296   Although particulate OM had a lower D/L ratio than dissolved OM (Fig. 6), it should be noted

297   that this does not imply that mean dissolved OM is more aged or degraded than particulate OM.

298   Riverine POM and DOM usually show different ages (Bianchi and Bauer, 2011), and this can be

299   influenced by selective desorption/adsorption of bacteria and related detritus between the particulate

300   and dissolved phases which can strongly modify the biomarker-indicated degradation status of OM

301   (Dittmar et al., 2001a).

302   **4.2 Different fate of bulk organic carbon and nitrogen**

303   Leaching of DOC and DON from peatlands is driven by different mechanisms: DOC release

304   is related to the status of peatland (pristine vs. degraded), whereas DON release is determined by

305   the DIN content of peatland soil (Kalbitz and Geyer, 2002). In the Rajang, bulk DOC and DON

306   concentrations were not coupled, as indicated by variations in DOC/DON ratios   (Fig. 7). The

307   average DOC concentration in the estuary part was slightly higher (345 μM) than in the river part

308   (337 μM; Table 3), suggesting the addition of DOC in the estuary. In comparison, there appears to

309   have been removal of DON in the estuary (Jiang et al., 2019).

310   In the Rajang, estuarine DOC exhibited non-conservative dilution behavior based on optical

311   properties (Martin et al., 2018), which is consistent with other peatland-draining rivers in Sarawak

312   (Müller et al., 2016). The contribution of marine sources to dissolved OM is reflected in the

313   increasing DOC-δ^{13}C in the estuary part (Fig. 3a). Peatland, however, is known for its high

314   contribution to fluvial DOC and has been suggested to contribute to the DOC in the Rajang (Martin

315   et al., 2018). In peatland-draining rivers west of the Rajang, the DOC concentration endmember can

316   be as high as 3690 μM (Müller et al., 2015). Under such high DOC background, a simple three-

317   point mixing model, with endmembers of (1) observed fluvial DOC concentration, (2) peatland

318   DOC concentration, and (3) inferred fluvial DOC concentration from a marine-river mixing curve,

319   suggested that peatland-DOC addition accounts for 3% of the fluvial DOC in the Saribas River and

320   15% in the Lupar River (Müller et al., 2016). Assuming that peatland in the Rajang estuary has a

321   comparable endmember DOC concentration to other peatland in Sarawak (i.e., 3690 μM; Müller et

al., 2015), and given our observed Rajang fresh water DOC endmember value of 337 μM (DOC

concentration at S5 station) and a marine DOC endmember of 238 μM (S1 station), a similar

mixing model approach suggests that peatland DOC contributed 4% of the Rajang fluvial DOC,

which is comparable to the Saribas River and much lower than the Lupar River (Müller et al., 2016).

In the meantime, as mentioned in the previous section, there is a non-conservative dilution pattern,

with dissolved OM in the estuary part more degraded than expected based on simple dilution with

a marine endmember (Figs. 4a & 5a). Hence it is reasonable that peatland not only contributed to

the fluvial DOC in concentration (Martin et al., 2018), but also modified the dissolved OM

composition (more bio-degraded) in the estuary. In another tropical river study, mangroves in the

estuary exerted a stronger influence on fluvial dissolved OM than hinterland vegetation (Dittmar et

al., 2001b). This is consistent with the Rajang, for which estuarine processes apparently impact the

dissolved OM in terms of both DOC concentration (by increasing the bulk amount) and composition

(by adding bio-degraded DOC). The estuarine dissolved OM showed higher bio-degraded

characteristics (e.g., elevated GABA% and D/L ratio; Figs. 4a&5a), but this subpart may be

photolabile (Martin et al., 2018). Photodegradation is expected to be enhanced when TSM decreases

and light penetration in the water column increases (e.g., as OM enters the sea) (Martin et al., 2018).

Other oceanic degradation mechanisms include the priming effect (Bianchi, 2011). The fate of the

terrestrial OM in the sea requires further study. As we lack the DON concentration endmember in

peatland, peatland impact on DON in the estuary was not estimated in the current study.

In contrast to DOC, which was apparently added to the estuary, DON was removed,

contributing to a remarkable increase of dissolved inorganic nitrogen in the estuary (Jiang et al.,

2019). In the fresh water section, the nitrate concentration was not related to the ratio of D/L

344   dissolved AAs, nor dissolved GABA% (Fig. 8). However, in the estuarine section, although nitrate

345   concentration was not related to D/L AAs, it   was related to GABA% (Fig. 8b). This indicates that

346   fluvial nitrate in the fresh water section was not derived from remineralization of fluvial organic

347   matter in the river channel, but more likely from other sources (e.g., leaching of soil). In the estuarine

348   section, some DON transformation may have occurred (Jiang et al., 2019), although leaching from

349   soils cannot be ruled out (Fig. 8). For the particulate phase, no relationship between nitrate and

350   particulate OM composition was detected (figure not shown).

351   The atomic DOC/DON ratio in the Rajang averaged 50 in the river part, and increased to 140

352   (mean value) in the estuary part (Fig. 7). Although the DOC/DON ratio was much higher than in

353   other tropical peatland river waters (around 10; Sjögersten et al., 2011), the ratio was comparable to

354   that in other peatland-draining rivers in Sarawak like the Lupar, Saruba and Maludan rivers (Müller

355   et al., 2015; Müller et al., 2016), which all enter the South China sea. The ratio is also within the

356   reported C/N ratio of peatland and leaves (Müller et al., 2016). For the Amazon River, the DOC to

357   total nitrogen ratio ranges from 27 to 52 (Hedges et al., 1994) and, given that this ratio includes

358   inorganic nitrogen, the DOC/DON ratio for the Amazon River would be even higher. Under the

359   background of such high C/N ratios (e.g., 50), transformation of DON to DIN in the estuary further

360   enhanced the high DOC/DON ratio (to 140), and hence a deficiency in terrestrial organic nitrogen

361   output is expected for the Rajang River. We noted that dissolved inorganic nitrogen concentrations

362   in the Rajang were on the order of 10 μM, comparable to DON (Jiang et al., 2019). Terrestrial

363   nitrogen output is an important source for coastal primary production (Jiang et al., 2019), but

364   peatland-impacted rivers may have relatively lower nitrogen input to the South China Sea when

365   compared with their very high river basin DOC yields (Baum et al., 2007). On one hand, logging

366 and secondary growth has been found to play a negative role in the nitrogen output efficiency of

367 forest soils (Davidson et al., 2007). On the other hand, disturbed tropical peatlands could release

368 more DOC in comparison to an undisturbed site (Moore et al., 2013) while the DOC/DON ratio

369 may also decrease along with disturbance of peatland (Kalbitz and Geyer, 2002). Given that

370 secondary growth in the river basin and anthropogenic disturbance of peatland (e.g., drainage and

371 conversion for oil palm) are both common (Hooijer et al., 2015), changes of DOC/DON ratios in

372 the Rajang are complex and further assessment is needed.

373

374 **5. Summary and Conclusion**

375   In August 2016 in the Rajang, we observed that dissolved OM composition (as D/L Glx ratio)

376 was conservatively diluted along with increasing DOC δ^{13}C, indicating that the sources of dissolved

377 OM have a very conservative impact on the OM composition. When D/L Glx ratios were plotted

378 against salinity, this linear conservative dilution pattern disappeared (Figs. 4a & 5a). This implies

379 that the total addition of DOC in the estuary (peatland/mangrove) had an impact on dissolved OM

380 composition, adding more bio-degraded OM, and resulting in data above the theoretical dilution

381 line (Figs. 4a & 5a). For particulate OM, though the data was variable, the overall decreasing GABA%

382 or D/L ratio with increasing salinity was much clearer relative to that of dissolved OM (Figs. 4b &

383 5b). Particulate D/L Glx ratio in the estuary was usually lower than in the fresh water section (Figs.

384 6b & c), whereas for dissolved OM, the majority of the samples in the estuary had a D/L Glx ratio

385 similar to of the fresh water section (Fig. 6a). The difference in OM composition between fresh

386 water and estuarine section suggests that dissolved OM became more degraded while particulate

387 OM became less degraded in the estuary.

388   The Rajang is characterized by DOC/DON ratios of 50 in the fresh water section, and the

389   further loss of DON in the estuary increased the ratio to 140. Peatland draining and

390   logging/secondary growth are reported to have conflicting impacts on carbon and nitrogen cycling

391   (Davidson et al., 2007; Moore et al., 2013), which may increase fluvial DOC and limit basin nitrogen

392   output, resulting in even larger DOC/DON ratios. Mismatch in carbon and nitrogen loss from

393   tropical rivers due to anthropogenic activities plays a role in material cycling in both terrestrial and

394   marine systems, enhancing the role of tropical rivers as direct sources of carbon to atmosphere; the

395   effect of changes in nitrogen output and its feedback on the carbon cycle needs further monitoring

396   and assessment.

397   Finally, this work is based on a dry season investigation (August). Though the seasonality for

398   Rajang OM may be moderate (Martin et al., 2018), for biomarkers like amino acids enantiomers

399   further investigation in the wet season is needed.

400

412

References

414   Amon, R. M. W., Fitznar, H. P., and Benner, R.: Linkages among the bioreactivity, chemical composition,

415   and diagenetic state of marine dissolved organic matter, Limnology and Oceanography, 46, 287-297,

416   2001.

417   Baum, A., Rixen, T., and Samiaji, J.: Relevance of peat draining rivers in central Sumatra for the riverine

418   input of dissolved organic carbon into the ocean, Estuarine, Coastal and Shelf Science, 73, 563-570,

419   2007.

420   Bianchi, T. S.: The role of terrestrially derived organic carbon in the coastal ocean: A changing paradigm

421   and the priming effect, Proceedings of the National Academy of Sciences, 108, 19473-19481, 2011.

422   Bianchi, T. S. and Bauer, J. E.: Particulate Organic Carbon Cycling and Transformation. In: Treatise on

423   Estuarine and Coastal Science, Editors-in-Chief: Eric, W. and Donald, M. (Eds.), Academic Press, Waltham,

424   2011.

425   Cifuentes, L. A., Coffin, R. B., Solorzano, L., Cardenas, W., Espinoza, J., and Twilley, R. R.: Isotopic and

426   Elemental Variations of Carbon and Nitrogen in a Mangrove Estuary   Estuarine Coastal and Shelf

427   Science, 43, 781-800, 1996.

428   Cloern, J. E., Foster, S. Q., and Kleckner, A. E.: Phytoplankton primary production in the world's

429   estuarine-coastal ecosystems, Biogeosciences, 11, 2477-2501, 2014.

430   Dauwe, B. and Middelburg, J. J.: Amino acids and hexosamines as indicators of organic matter

431   degradation state in North Sea sediments, Limnology and Oceanography, 43, 782-798, 1998.

432   Davidson, E. A., de Carvalho, C. J. R., Figueira, A. M., Ishida, F. Y., Ometto, J. P. H. B., Nardoto, G. B., Saba,

433   R. T., Hayashi, S. N., Leal, E. C., Vieira, I. C. G., and Martinelli, L. A.: Recuperation of nitrogen cycling in

434   Amazonian forests following agricultural abandonment, Nature, 447, 995-998, 2007.

435   Davis, J., Kaiser, K., and Benner, R.: Amino acid and amino sugar yields and compositions as indicators

436   of dissolved organic matter diagenesis, Organic Geochemistry, 40, 343-352, 2009.

437   Dittmar, T., Fitznar, H. P., and Kattner, G.: Origin and biogeochemical cycling of organic nitrogen in the

438   eastern Arctic Ocean as evident from D- and L-amino acids, Geochimica et Cosmochimica Acta, 65,

439   4103-4114, 2001a.

440   Dittmar, T., Lara, R. J., and Kattner, G.: River or mangrove? Tracing major organic matter sources in

441   tropical Brazilian coastal waters, Marine Chemistry, 73, 253-271, 2001b.

442   Fitznar, H. P., Lobbes, J. M., and Kattner, G.: Determination of enantiomeric amino acids with high-

443   performance liquid chromatography and pre-column derivatisation with o-phthaldialdehyde and N-

444   isobutyrylcysteine in seawater and fossil samples (mollusks), Journal of Chromatography A, 832, 123-

445   132, 1999.

446   Gandois, L., Teisserenc, R., Cobb, A. R., Chieng, H. I., Lim, L. B. L., Kamariah, A. S., Hoyt, A., and Harvey,

447   C. F.: Origin, composition, and transformation of dissolved organic matter in tropical peatlands,

448   Geochimica et Cosmochimica Acta, 137, 35-47, 2014.

449   Hedges, J. I., Cowie, G. L., Richey, J. E., Quay, P. D., Benner, R., Mike, S., and Forsberg, B. R.: Origins and

450   processing of organic matter in the Amazon River as indicated by carbohydrates and amino acids,

451   Limnology and Oceanography, 39, 743-761, 1994.

452 Hedges, J. I. and Man, D. C.: The characterization of plant tissues by their lignin oxidation products,
453 Geochimica et Cosmochimica Acta, 43, 1803-1807, 1979.

454 Hernes, P. J., Robinson, A. C., and Aufdenkampe, A. K.: Fractionation of lignin during leaching and
455 sorption and implications for organic matter "freshness", Geophysical Research Letters, 34, 2007.

456 Hooijer, A., Vernimmen, R., Visser, M., and Mawdsley, N.: Flooding projections from elevation and
457 subsidence models for oil palm plantations in the Rajang delta peatlands, Sarawak, Malaysia, Deltares
458 report 1207384, 76 pp., 2015.

459 Huang, T. H., Chen, C. T. A., Tseng, H. C., Lou, J. Y., Wang, S. L., Yang, L., Kandasamy, S., Gao, X., Wang, J.
460 T., Aldrian, E., Jacinto, G. S., Anshari, G. Z., Sompongchaiyakul, P., and Wang, B. J.: Riverine carbon fluxes
461 to the South China Sea, Journal of Geophysical Research: Biogeosciences, 122, 1239-1259, 2017.

462 Jennerjahn, T. C., Ittekkot, V., Klöpper, S., Adi, S., Purwo Nugroho, S., Sudiana, N., Yusmal, A., Prihartanto,
463 and Gaye-Haake, B.: Biogeochemistry of a tropical river affected by human activities in its catchment:
464 Brantas River estuary and coastal waters of Madura Strait, Java, Indonesia, Estuarine, Coastal and Shelf
465 Science, 60, 503-514, 2004.

466 Jiang, S., Müller, M., Jin, J., Wu, Y., Zhu, K., Zhang, G., Mujahid, A., Rixen, T., Muhamad, M. F., Sia, E. S.
467 A., Jang, F. H. A., and Zhang, J.: Dissolved inorganic nitrogen in a tropical estuary at Malaysia: transport
468 and transformation, Biogeosciences Discuss., 2019, 1-27, 2019.

469 Kaiser, K. and Benner, R.: Biochemical composition and size distribution of organic matter at the Pacific
470 and Atlantic time-series stations, Marine Chemistry, 113, 63-77, 2009.

471 Kaiser, K. and Benner, R.: Hydrolysis-induced racemization of amino acids, Limnology and Oceanography:
472 Methods, 3, 318-325, 2005.

473 Kalbitz, K. and Geyer, S.: Different effects of peat degradation on dissolved organic carbon and nitrogen,
474 Organic Geochemistry, 33, 319-326, 2002.

475 Kimber, R. W. L., Nannipieri, P., and Ceccanti, B.: The degree of racemization of amino acids released by
476 hydrolysis of humic-protein complexes: Implications for age assessment, Soil Biology and Biochemistry,
477 22, 181-185, 1990.

478 Lamade, E., Setiyo, I. E., Girard, S., and Ghashghaie, J.: Changes in 13C/12C of oil palm leaves to
479 understand carbon use during their passage from heterotrophy to autotrophy, Rapid Communications
480 in Mass Spectrometry, 23, 2586-2596, 2009.

481 Lamb, A. L., Wilson, G. P., and Leng, M. J.: A review of coastal palaeoclimate and relative sea-level
482 reconstructions using δ13C and C/N ratios in organic material, Earth-Science Reviews, 75, 29-57, 2006.

483 Martin, P., Cherukuru, N., Tan, A. S. Y., Sanwlani, N., Mujahid, A., and Müller, M.: Distribution and cycling
484 of terrigenous dissolved organic carbon in peatland-draining rivers and coastal waters of Sarawak,
485 Borneo, Biogeosciences, 15, 6847-6865, 2018.

486 Mayorga, E., Aufdenkampe, A. K., Masiello, C. A., Krusche, A. V., Hedges, J. I., Quay, P. D., Richey, J. E.,
487 and Brown, T. A.: Young organic matter as a source of carbon dioxide outgassing from Amazonian rivers,
488 Nature, 436, 538-541, 2005.

489 Moore, S., Evans, C. D., Page, S. E., Garnett, M. H., Jones, T. G., Freeman, C., Hooijer, A., Wiltshire, A. J.,
490 Limin, S. H., and Gauci, V.: Deep instability of deforested tropical peatlands revealed by fluvial organic
491 carbon fluxes, Nature, 493, 660, 2013.

492 Müller-Dum, D., Warneke, T., Rixen, T., Müller, M., Baum, A., Christodoulou, A., Oakes, J., Eyre, B. D., and
493 Notholt, J.: Impact of peatlands on carbon dioxide (CO2) emissions from the Rajang River and Estuary,
494 Malaysia, Biogeosciences, 16, 17-32, 2019.

495 Müller, D., Warneke, T., Rixen, T., Müller, M., Jamahari, S., Denis, N., Mujahid, A., and Notholt, J.: Lateral

496 carbon fluxes and CO2 outgassing from a tropical peat-draining river, Biogeosciences, 12, 5967-5979,
497 2015.

498 Müller, D., Warneke, T., Rixen, T., Müller, M., Mujahid, A., Bange, H. W., and Notholt, J.: Fate of terrestrial
499 organic carbon and associated CO2 and CO emissions from two Southeast Asian estuaries,
500 Biogeosciences, 13, 691-705, 2016.

501 Raymond, P. A. and Bauer, J. E.: Use of 14C and 13C natural abundances for evaluating riverine, estuarine,
502 and coastal DOC and POC sources and cycling: a review and synthesis, Organic Geochemistry, 32, 469-
503 485, 2001.

504 Schleifer, K. H. and Kandler, O.: Peptidoglycan types of bacterial cell walls and their taxonomic
505 implications, Bacteriological Reviews, 36, 407-477, 1972.

506 Schroeder, R. A. and Bada, J. L.: A review of the geochemical applications of the amino acid racemization
507 reaction, Earth-Science Reviews, 12, 347-391, 1976.

508 Sjögersten, S., Cheesman, A. W., Lopez, O., and Turner, B. L.: Biogeochemical processes along a nutrient
509 gradient in a tropical ombrotrophic peatland, Biogeochemistry, 104, 147-163, 2011.

510 Vollmer, W., Blanot, D., and de Pedro, M.: Peptidoglycan structure and architecture, FEMS Microbiology
511 Review, 32, 149-167, 2008.

512 Wu, Y., Zhu, K., Zhang, J., Müller, M., Jiang, S., Mujahid, A., Muhamad, M. F., and Sia, E. S. A.: Distribution
513 and degradation of terrestrial organic matter in the sediments of peat-draining rivers, Sarawak,
514 Malaysian Borneo, Biogeosciences Discuss., 2019, 1-37, 2019.

515 Zhang, C. L., Dang, H. Y., Azam, F., Benner, R., Legendre, L., Passow, U., Polimene, L., Robinson, C., Suttle,
516 C. A., and Jiao, N. Z.: Evolving paradigms in biological carbon cycling in the ocean, National Science
517 Review, 5, 481-499, 2018.

518 Zhu, Z. Y., Wu, Y., Zhang, J., Dittmar, T., Li, Y., Shao, L., and Ji, Q.: Can primary production contribute non-
519 labile organic matter in the sea: Amino acid enantiomers along the coast south of the Changjiang
520 Estuary in May, Journal of Marine Systems, 129, 343-349, 2014.

521 Zhu, Z. Y., Zhang, J., Wu, Y., and Lin, J.: Bulk particulate organic carbon in the East China Sea: Tidal
522 influence and bottom transport, Progress in Oceanography, 69, 37-60, 2006.

523
524

525 Table 1. Measured amino acids (the L- and D- enantiomers are not listed) and all abbreviations in
526 this study. Note that glycine has no enantiomer.

name	abbreviations
organic matter	OM
dissolved organic carbon	DOC
dissolved organic nitrogen	DON
total suspended matter	TSM
amino acid	AA
total hydrolysable dissolved amino acids	TDAA
total hydrolysable particulate amino acids	TPAA
Alanine	Ala
Arginine	Arg
Asparagine	Asx
Aspartic acid	
Glutamine	Glx
Glutamic acid	
Glycine	Gly
Isoleucine	Ile
Leucine	Leu
Lysine	Lys
Methionine	Met
Phenylalanine	Phe
Serine	Ser
Threonine	Thr
Tryptophan	Trp
Tyrosine	Tyr
Valine	Val
γ - aminobutyric acid	GABA

527
528

529 Table 2. TSM, DOC, POC and stable carbon isotopes in the freshwater and estuary of the Rajang
530 (mean (min-max)).
531

	unit	Fresh water	Estuary
TSM	mg/L	61 (22 - 126)	73 (25 - 161)
DOC	μM	337 (217 - 658)	345 (214 - 587)
DOC δ^{13}C	‰	−26.7 (−27.7 - −25.0)	−26.1 (−28.7 - −20.1)
POC	μM	86 (46 - 125)	64 (22 - 153)
	%	1.9 (1.2 - 2.5)	1.0 (0.6 - 1.9)
POC δ^{13}C	‰	−30.1 (−31.1 - −29.4)	−26.7 (−30.1 - −23.8)

532
533
534
535

536 Table 3 Rajang AAs (mean (min-max)) in August 2016 (*Total D/TDAA = total D form AA versus
537 TDAA. Total D/TPAA = total D form AA versus TPAA)
538

		unit	Fresh water	Estuary
dissolved	TDAA	nM	317 (131 - 486)	523 (212 - 2320)
	TDAA carbon yield	%	0.40 (0.08 - 0.65)	0.38 (0.29 - 0.53)
	TDAA nitrogen yield	%	4.8 (1.3 - 15)	11 (5.4 - 18)
	GABA	%	2.0 (1.3 - 4.1)	1.3 (0.15 - 1.9)
	total D/total TDAA*	%	12 (8 - 15)	12 (3 - 14)
	D/L Glx		0.35 (0.16 - 0.57)	0.32 (0.07 - 0.42)
	D/L Asx		0.34 (0.23 - 0.48)	0.34 (0.08 - 0.42)
particulate	TPAA	μM	2.5 (1.4 - 3.6)	2.0 (1.1 - 3.7)
	TPAA carbon yield	%	14 (9.5 - 19)	17 (11 - 24)
	TPAA nitrogen yield	%	66 (36 - 82)	62 (30 - 100)
	GABA%	%	0.7 (0.6 - 0.9)	0.4 (0.2 - 0.8)
	total D/total TPAA*	%	4.4 (3.6 - 5.2)	3.3 (2.4 - 5.0)
	D/L Glx		0.09 (0.08 - 0.10)	0.06 (0.04 - 0.08)
	D/L Asx		0.04 (0.03 - 0.05)	0.05 (0.03 - 0.11)

539
540

Figure caption

Figure 1. Study area and sampling stations. a) Location of Sarawak, Malaysia; and b) the Rajang with its estuary/river mouth shown. Samples upstream of S5 had 0 salinity and downstream of S5 had salinity >0. Hence, from S5 to S10 was regarded as the fresh water section (red triangles), and downstream of S5 was regarded as the estuarine section (blue triangles). Note that salinity of samples at S15, S17, S18, S19 was also 0 during our sampling.

Figure 2. Distribution patterns of (a) TSM, (b) DOC and (c) POC along with salinity in the Rajang. The fresh water data point represents all samples with salinity = 0 and the error bar corresponds to the standard deviation. The marine data point represents S1.

Figure 3. Distribution patterns of (a) DOC δ^{13}C and (b) POC δ^{13}C along with conductivity/salinity in the Rajang. The legend indicates the branches that the samples were collected from and the marine data points correspond to station S1.

Figure 4. The GABA% distribution pattern from fresh water to the estuary in the Rajang: a) dissolved and b) particulate. Note the different x-axis scales between plot a and b. The dashed line indicates the linear mixing line between fresh and marine endmembers. The fresh water endmember (brown triangle) was calculated as the mean of all fresh water samples (salinity = 0), and the marine endmember (purple diamond) was calculated as the mean of all offshore samples with salinity >30. The error bar indicates the standard deviation.

Figure 5. The D/L Glx distribution pattern from fresh water to the estuary in the Rajang: a) dissolved and b) particulate. Note the different x-axis scales between plot a and b. The dashed line indicates the linear mixing line between fresh and marine endmembers. The fresh water endmember (brown triangle) was calculated as the mean of all fresh water samples (salinity = 0), and the marine endmember (purple diamond) was calculated as the mean of all offshore samples with salinity >30. The error bar indicates the standard deviation.

Figure 6. D/L ratio of AAs (as Glx) plotted against a) DOC δ^{13}C b) POC δ^{13}C, and c) PN δ^{15}N.

Figure 7. DOC/DON ratio distribution pattern along with salinity in the Rajang. For fresh water and estuary, the mean DOC/DON value was 50 and 140, respectively. DON concentrations are taken from Jiang et al., (2019).

Figure 8. Dissolved OM composition (a: D/L Glx, b: GABA%) and its relationship with nitrate concentration. Nitrate concentrations are taken from Jiang et al., (2019).
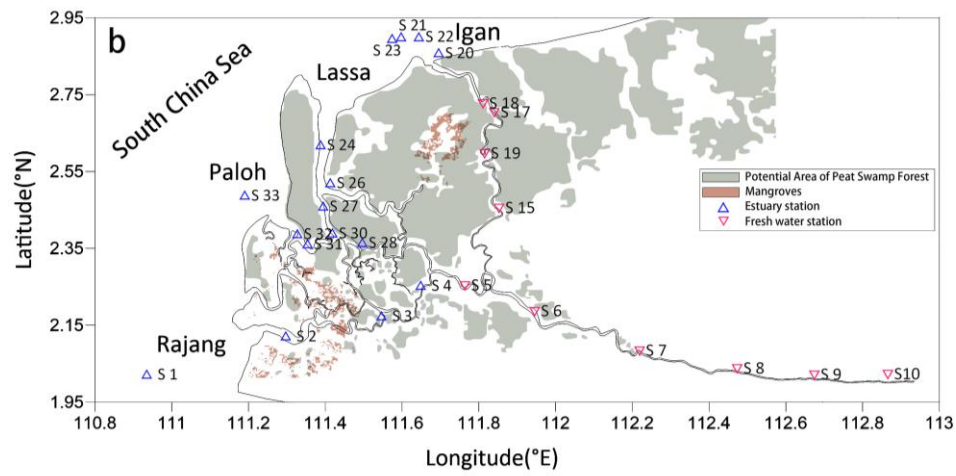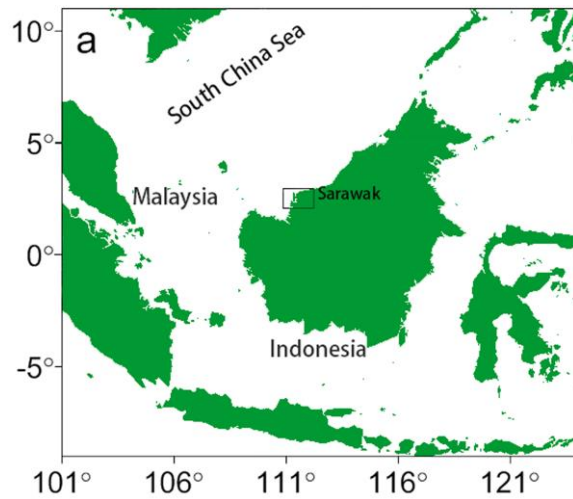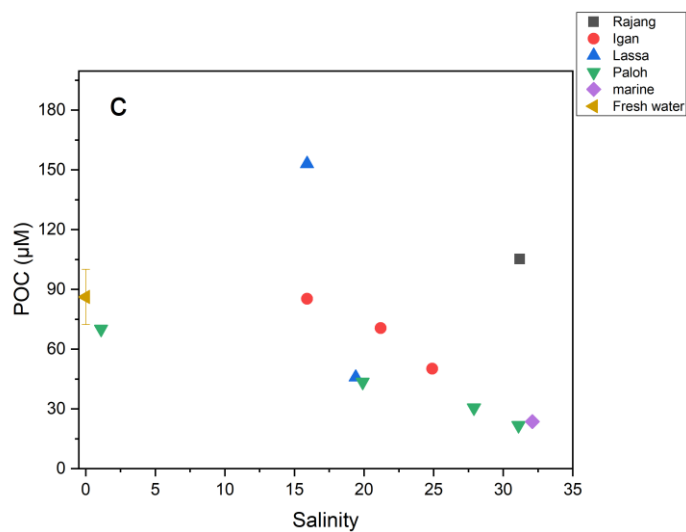
575

576
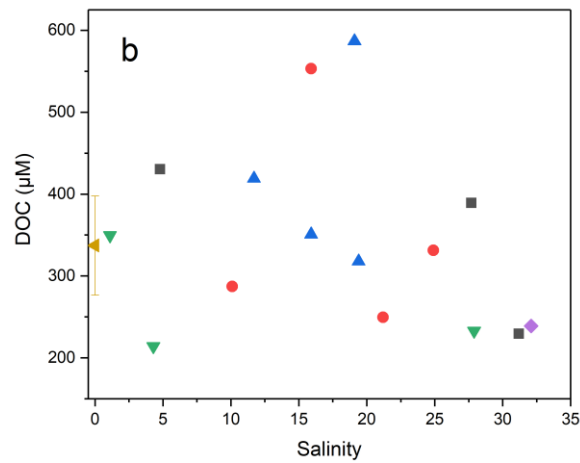
577 Figure 1.

578

579

580

581

582

583

584   Figure 2.

585

586

588   Figure 3.

589

590

591

592

593

594   Figure 4.

595

596

597

598   Figure 5.

599

600

601

602

603

Figure 6.

604

605

606

607

608

609   Figure 7.

610

611

612

613

614

615

616

617   Figure 8.